ELECTROWEAK RESULTS FROM THE Z RESONANCE CROSS-SECTIONS AND LEPTONIC FORWARD-BACKWARD ASYMMETRIES WITH THE ALEPH DETECTOR

E. TOURNEFIER
CERN, Switzerland
E-mail: Edwige.Tournefier@cern.ch

The measurement of the Z resonance parameters and lepton forward-backward asymmetries are presented. These are determined from a sample of 4.5 million Z decays accumulated with the ALEPH detector at LEP I.

1 Introduction

From 1990 to 1995 the LEP e^+e^- storage ring was operated at centre of mass energies close to the Z mass, in the range $|\sqrt{s} - M_Z| < 3$ GeV. Most of the data have been recorded at the maximum of the resonance (120 pb^{-1} per experiment) and about 2 GeV below and above (40 pb^{-1} per experiment).

The measurement of the hadronic and leptonic cross sections as well as the leptonic forward backward asymmetries performed with the ALEPH detector at these energies are presented here. The large statistic allows a precise measurement of these quantities which are then used to determine the Z lineshape parameters: the Z mass M_Z, the Z width Γ_Z, the total hadronic cross section at the pole σ^0_{had} and the ratio of hadronic to leptonic pole cross sections $R_l = \sigma^0_{had}/\sigma^0_l$.

Here we will give some details of the ALEPH experimental measurement of these quantities. A review of the whole LEP electroweak measurements and a discussion of the results as a test of the Standard Model can be found in another talk of this conference [1].

2 Cross sections and leptonic Forward-Backward asymmetries measurement

The cross section and asymmetries are determined for the s-channel process $e^+e^- \to Z, \gamma \to f\bar{f}$. The cross section is derived from the number of selected events N_{sel} with

$$\sigma_{f\bar{f}} = \frac{N_{sel}(1 - f_{bkg})}{\epsilon} \frac{1}{\mathcal{L}} \qquad (1)$$

where f_{bkg} is the fraction of background, ϵ is the selection efficiency and $\mathcal{L}$ is the integrated luminosity. Note that in the case of e^+e^- final state the irreducible background originating from the exchange of γ (Z) in the t-channel is subtracted from N_{sel} to obtain the s-channel cross section.

The leptonic forward-backward asymmetry (A_{FB}) is derived from a fit to the angular distribution

$$\frac{d\sigma_{f\bar{f}}}{d\cos\theta^*} \propto 1 + \cos^2\theta^* + \frac{8}{3}A_{FB}\cos\theta^* \quad (2)$$

where θ^* is the centre of mass scattering angle between the incoming e^- and the out-coming negative lepton.

To achieve a good precision on the cross section a high efficiency and low background is necessary while the asymmetry is insensitive to the overall efficiency and to a background with the same asymmetry as the signal. This justifies the use of different leptonic selections for cross section and asymmetry measurement.

2.1 Hadronic cross sections

Four million of $e^+e^- \to q\bar{q}$ events have been recorded at the Z peak, leading to a statistical uncertainty of 0.05%. The systematic uncertainty has been reduced to the same level.

The hadronic cross section measurement is based on two independent selections. The first selection is based on charged track properties while the second is based on calorimetric energy. Details of these selections can be found in previous publications [2]. These two measurements are in good agreement and are combined to obtain the final result. The systematic uncertainties of these selections are almost uncorrelated because they are mainly based on uncorrelated quantities therefore the combination of the 2 selections allows to reduce the systematic uncertainty.

Figure 1 shows the distribution of charged multiplicity versus the charged track energy for signal and background. These variables are used to separate $e^+e^- \to q\bar{q}$ events from background in the charged track selection. The most dangerous background in both selections is $\gamma\gamma$ events because Monte Carlo prediction is not fully reliable. Therefore a method to determine this background from the data has been developed. This is achieved by exploiting the different $\sqrt{s}$ dependence of the resonant (signal) and non-resonant (background) contributions. The resultant systematic error (0.04%) reflects the statistic of the data.

The dominant systematic error in the calorimetric selection comes from the calibration of calorimeters (0.09%) and, in the charged track selection

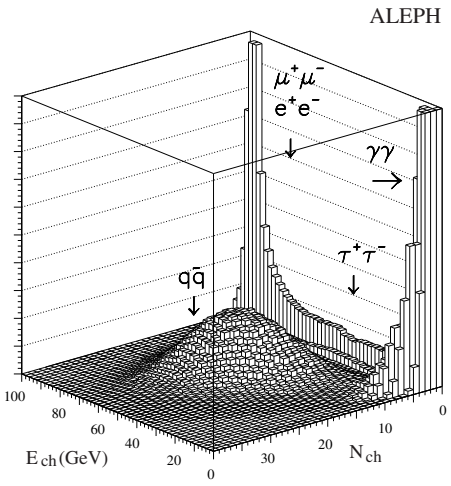

Figure 1. Distribution of charged track multiplicity (N_{ch}) versus charged track energy (E_{ch}).

Table 1. Efficiency, background and systematic errors for the two hadronic selections at the peak point.

	Charged tracks	Calorimeter
Efficiency (%)	97.48	99.07
Background (%)		
$\tau^+\tau^-$	0.32	0.44
$\gamma\gamma$	0.26	0.16
e^+e^-	-	0.08
Systematic (%)		
Detector simulation	0.02	0.09
Hadronisation modelling	0.06	0.03
$\tau^+\tau^-$ bkg	0.03	0.05
$\gamma\gamma$ bkg	0.04	0.03
e^+e^- bkg	-	0.03
Total syst.	0.087	0.116
Combined	0.071	

from the determination of the acceptance (0.06%). Table 1 gives a breakdown of the efficiency, the background and the systematic uncertainties of both selections.

2.2 Leptonic cross sections

The statistical uncertainty in the leptonic channel is of the order of 0.15%, The aim of the analysis is to reduce the systematic to less than 0.1%. Two analyses were developed for the measurement of the leptonic cross sections. The first one, referred to as *exclusive* is based on three independent selections each aimed at isolating one lepton flavour and still follows the general philosophy of the analysis procedures described earlier [2]. The second one is new and has been optimised for the measurement of R_l, it is refered as *global* di-lepton selection. The results of these selections agree within the uncorrelated statistical error and have been combined for the final result. These selections are not independent since they make use of similar variables therefore their combination does not reduce the systematic uncertainty.

We concentrate here on the *global* analysis. This selection takes advantage of the excellent particle identification capabilities (dE/dx, shower developement in the calorimeters and muon chamber information) and the high granularity of the ALEPH detector. First di-leptons are selected within the detector acceptance with an efficiency of 99.2% and the background arising from $\gamma\gamma$, $q\bar{q}$ and cosmic events is reduced to the level of 0.2%. Then the lepton flavour separation is performed inside the di-lepton sample so that the systematic uncertainties are anti-correlated between 2 lepton species and that no additional uncertainty is introduced on R_l. Table 2 gives a breakdown of the systematic errors obtained with 1994 data. The background from $q\bar{q}$ and $\gamma\gamma$ events affects mainly the $\tau^+\tau^-$ channel, therefore this channel is affected by bigger selection systematics than e^+e^- and $\mu^+\mu^-$.

As an example we consider the systematic errors related to the $\tau^+\tau^-$ selection efficiency. This efficiency is measured on the data: $\tau^+\tau^-$ events are selected using tight selection criteria to flag τ-like hemispheres; with the sample of opposite hemispheres, *artificial* $\tau^+\tau^-$ events are constructed by associating two back-to-back such hemispheres and the selection cuts are applied. In order to assess the validity of the method and to correct for possible bias of this method, two different Monte Carlo reference samples are used. On the first sample the same procedure of artificial $\tau^+\tau^-$ events is applied, on the second one the selection cuts are applied directly. The uncertainty on the efficiency measured with this method is dominated by the statistic of the artificial events used in the data. This method is applied in order to measure

Table 2. Systematic uncertainties in percent of dilepton cross sections for peak 1994 data. Correlations between lepton flavours are taken into account in the l^+l^- column.

	e^+e^-	$\mu^+\mu^-$	$\tau^+\tau^-$	l^+l^-
Global selection				
Tracking efficiency	0.05	0.03	0.03	0.04
Angles measurement (*)	0.02	0.01	0.01	0.02
ISR and FSR simulation (*)	0.03	0.03	0.03	0.03
$\gamma\gamma$ cuts (*)	0.02	-	0.05	0.02
$q\bar{q}$ cuts	-	-	0.11	0.04
$\gamma\gamma$ background (*)	-	-	0.02	-
$q\bar{q}$ background(*)	-	-	0.04	0.01
Flavour separation				
$\mu^+\mu^-/\tau^+\tau^-$	-	0.03	0.03	-
$e^+e^-/\tau^+\tau^-$				
$cos\theta^* < 0.7$	0.08	-	0.07	0.01
$cos\theta^* \geq 0.7$	-	-	0.06	0.02
t-channel subtraction				
(*)	0.11	-	-	0.04
Monte Carlo statistic				
	0.05	0.06	0.07	0.04
Total	0.16	0.08	0.19	0.09

(*)uncertainties completely correlated among all energy points.

the inefficiency arising from $q\bar{q}$ cuts and in the flavour separation.

The dominant systematic in e^+e^- channel arises from t-channel subtraction and is given by the theoretical uncertainty [3] on the t-channel contribution to the cross section.

This leptonic cross section measurement contributes to a systematic uncertainty on R_l of 0.08%.

2.3 Leptonic Forward-Backward asymmetries

The measurement of the asymmetries is dominated by the statistical uncertainty equal to 0.0015. Special muon and tau selections have been designed for the asymmetry measurement while the e^+e^- *exclusive* selection is used for the e^+e^- asymmetry measurement. The e^+e^- angular distribution needs to be corrected for efficiency before subtracting the t-channel and therefore relies on Monte Carlo while $\mu^+\mu^-$ and $\tau^+\tau^-$ angular distributions do not need to

be corrected with Monte Carlo since the selections are designed so that the efficiency is symmetric.

Because of the $\gamma - Z$ interference, the asymmetry varies rapidly with the centre of mass energy $\sqrt{s'}$ around the Z mass. Cuts on energy induce a dependence of the efficiency with $\sqrt{s'}$ and therefore could introduce a bias in the measurement since the efficiency would no more be symmetric. To minimise these effects the selections are mainly based on particle identification instead of kinematic variables. Figure 2 shows the particle identification efficiency as

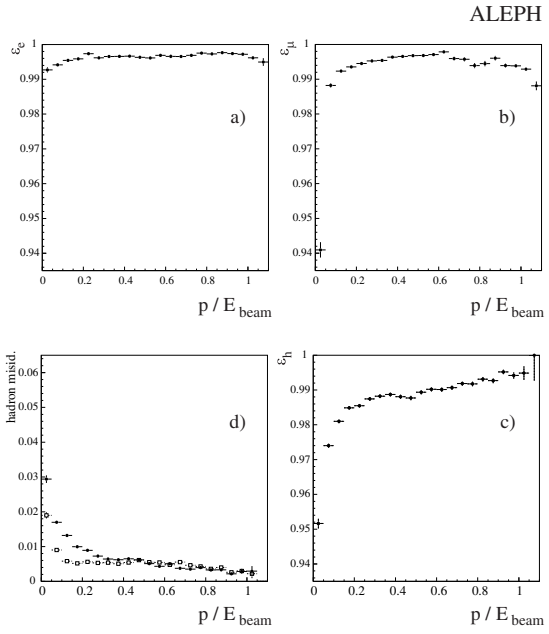

Figure 2. Identification efficiencies for a) electrons, b) muons and c) pions as a function of the momentum to the beam energy ratio. In d) the probability for a pion to be misidentified as an electron (squares) or a muon (circles) is shown.

a function of energy.

The asymmetry is extracted by performing a maximum likelihood fit to the differential cross section. The dominant systematic uncertainty arises from t-channel subtraction in the Bhabha channel (0.0013 on $A_{FB}^{0,e}$) and other systematic errors are smaller than 0.0005.

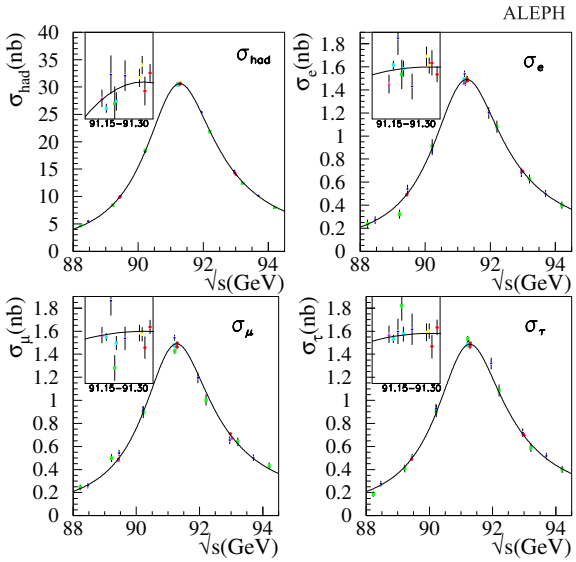

Figure 3. Measurement of cross sections. The inserts show enlarged views of the peak region.

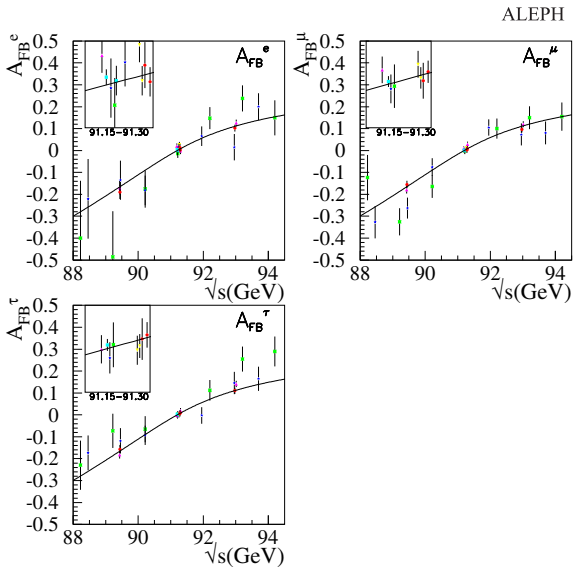

Figure 4. Measurement of the asymmetries. The inserts show enlarged views of the peak region.

Table 3. Result of the fit to experimental measurement of cross sections and leptonic forward-backward asymmetries. The total error is splitted into statistical and systematic errors, theoretical error on luminosity and on t-channel and LEP beam energy measurement error.

	value	stat	exp	lumi	t-ch	E_{beam}
M_Z	91.1883±0.0031	0.0024	0.0002			0.0017
Γ_Z	2.4953±0.0043	0.0038	0.0009			0.0013
σ^0_{had}	41.557±0.058	0.030	0.026	0.025		0.011
$R_e l$	20.677±0.075	0.062	0.033		0.025	0.013
R_μ	20.802±0.056	0.053	0.021			0.006
R_τ	20.710±0.062	0.054	0.033			0.006
$A^{0,e}_{FB}$	0.0189±0.0034	0.0031	0.0006		0.0013	0.0002
$A^{0,\mu}_{FB}$	0.0171±0.0024	0.0024	0.0005			0.0002
$A^{0,\tau}_{FB}$	0.0169±0.0028	0.0026	0.0011			0.0002
R_l	20.728±0.039	0.033	0.020		0.005	0.002
$A^{0,l}_{FB}$	0.0173±0.0016	0.0015	0.0004		0.0002	0.0001

3 Results

Figures 3 and 4 show the measured cross sections and asymmetries. The Z lineshape parameters are fitted to these measurements with the latest version of ZFITTER [4]. The error matrix used in the χ^2 fit includes the experimental statistic and systematic uncertainties, the LEP beam energy measurement uncertainty and the theoretical uncertainties arising from the small angle Bhabha cross section in the luminosity determination and the t-channel contribution to wide angle Bhabha events. The results are shown in Table 3.

The value of the Z couplings to charged leptons $|g_V|$ and $|g_A|$ can be derived from these parameters. The experimental measurement is shown in Figure 5 with the Standard Model prediction. The data favor a light Higgs.

The value of α_s can also be extracted from R_l, Γ_Z and σ^0_{had}:

$$\alpha_s = 0.115 \pm 0.004_{exp} \pm 0.002_{QCD} \quad (3)$$

where the first error is experimental and the second reflects uncertainties on the QCD part of the theoretical prediction [6]. Here the Higgs mass has been fixed to 150 GeV and the dependence of α_s with M_H can be approximately parametrised by $\alpha_s(M_H) = \alpha_s(M_H = 150\text{GeV}) \times (1 + 0.02 \times \ln(M_H/150))$ where M_H is expressed in GeV.

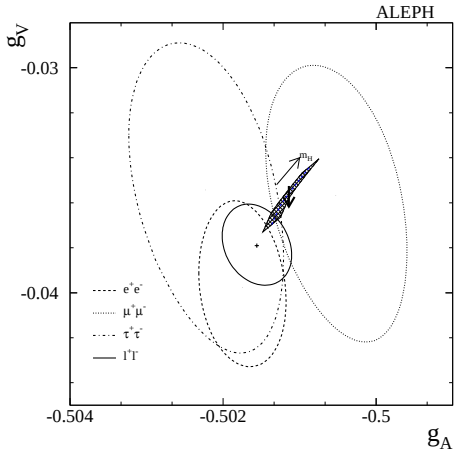

Figure 5. Effective lepton couplings. Shown are the one-σ contours. The shaded area indicates the Standard Model expectation for $M_t = 174 \pm 5$ GeV/c^2 and $90 < M_H GeV/c^2 < 1000$; the vertical fat arrow shows the change if the electromagnetic coupling constant is varied within its error. The sign of the couplings were assigned in agreement with τ polarisation measurements and neutrino data scattering.

4 Conclusion

The high statistic accumulated by ALEPH during LEP 1 running allows to measure the hadronic and leptonic cross sections and the leptonic forward-backward asymmetries with statistical and systematic precision of the order of 1 permil. These measurements are turned into precise determination of the Z boson properties and constraints on the Standard Model parameters.

Acknowledgments

I would like to thank D. Schlatter for his help in preparing this talk. I also would like to thank the organisers of the Lake Louise Winter Institute conference for the interesting program and the nice atmosphere at the conference.

References

1. talk given by J.Pinfold at this conference, to appear in these proceedings.

2. ALEPH Collaboration, Z.Phys. **C48** (1990) 365;
ALEPH Collaboration, Z.Phys. **C53** (1992) 1;
ALEPH Collaboration, Z.Phys. **C60** (1993) 71;
ALEPH Collaboration, Z.Phys. **C62** (1994) 539.
3. W. Beenakker, F.A. Berends and S.C. van der Marck, "Large Angle Bhabha Scattering", Nucl. Phys. **B349**(1991) 223;
W. Beenakker, G. Passarino, "Large Angle Bhabha Scattering at LEP1", Phys.Lett.B425:199-207,1998.
4. D. Bardin *et al.*, Z. Phys. **C44** (1989) 493; Comp. Phys. Comm. **59** (1990) 303; Nucl. Phys. **B351**(1991) 1; Phys. Lett. **B255** (1991) 290 and CERN-TH 6443/92 (May 1992)
newline recently updated with results from [5], from A. Czarnecki and J.H. Kühn, "Nonfactorizable QCD and Electroweak Corrections to the Hadronic Z Boson Decay Rate", hep-ph/9608366 preprint, (Aug. 1996), from G. Montagna et al."On the QED radiator at order α^3", preprint hep-ph/9611463, and from G. Degrassi, P. Gambino and A. Vicini, Phys. Lett. **B383** (1996) 219 and G. Degrassi, P. Gambino and A. Sirlin, Phys. Lett. **B394** (1997) 188.
5. *Reports of the working group on precision calculations for the Z resonance*, eds. D. Bardin, W. Hollik and G. Passarino, CERN Yellow Report 95-03, Geneva, 31 March 1995. and references therein.
6. T. Hebbeker, M. Martinez, G. Passarino and G. Quast, Phys. Lett. **B331** (1994) 165, and references therein.